Acta Oncologica

ISSN: 0284-186X (Print) 1651-226X (Online) Journal homepage: http://www.tandfonline.com/loi/ionc20

Intra- and inter-fraction uncertainties during IGRT for Wilms' tumor

Filipa Guerreiro, Enrica Seravalli, Geert O. Janssens, Cees P. van de Ven, Marry M. van den Heuvel-Eibrink & Bas W. Raaymakers

To cite this article: Filipa Guerreiro, Enrica Seravalli, Geert O. Janssens, Cees P. van de Ven, Marry M. van den Heuvel-Eibrink & Bas W. Raaymakers (2018) Intra- and inter-fraction uncertainties during IGRT for Wilms' tumor, Acta Oncologica, 57:7, 941-949, DOI: 10.1080/0284186X.2018.1438655

To link to this article: https://doi.org/10.1080/0284186X.2018.1438655

ACTA ONCOLOGICA
2018, VOL. 57, NO. 7, 941–949
https://doi.org/10.1080/0284186X.2018.1438655

Taylor & Francis
Taylor & Francis Group

ORIGINAL ARTICLE

Intra- and inter-fraction uncertainties during IGRT for Wilms' tumor

Filipa Guerreiro[a], Enrica Seravalli[a], Geert O. Janssens[b,c], Cees P. van de Ven[c], Marry M. van den Heuvel-Eibrink[c] and Bas W. Raaymakers[a]

[a]Department of Radiotherapy, University Medical Center Utrecht, Utrecht, The Netherlands; [b]Department of Radiation Oncology, University Medical Center Utrecht, Utrecht, The Netherlands; [c]Princess Máxima Center for Paediatric Oncology, Utrecht, The Netherlands

ABSTRACT

Background and purpose: To assess intra- and inter-fraction motion uncertainties, due to displacements of the tumor bed (TB) and organs at risk (OAR), as well as intra- and inter-fraction patient set-up uncertainties, due to positioning variations, during image-guided radiation therapy (IGRT) in children with Wilms' tumor.

Material and methods: Four-dimensional computed tomography (4D-CT) and daily pre- and post-treatment cone-beam CT (CBCT)-scans of 15 patients (average 4, range 1–8 years) undergoing flank irradiation after nephrectomy were analyzed. TB (marked by four surgical clips) and OAR motion uncertainties were quantified by displacements of the center of mass in all orthogonal directions. Translational and rotational bone off-sets were recorded for patient set-up uncertainties assessment in all orthogonal directions. The average results, systematic and random errors were computed.

Results: Average intra- and inter-fraction motion uncertainties were $\leq$1.1 mm (range: [−6.9;7.9] mm) for the TB and $\leq$3.2 mm (range: [−9.1;9.6] mm) for the OAR. Average intra- and inter-fraction patient set-up uncertainties were $\leq$0.1 mm (range: [−3.3;4.8] mm) and $\leq$0.9° (range: [0.0;2.8°]). Both motion and patient set-up uncertainties were larger for the cranio-caudal direction. Calculated systematic and random errors were $\leq$2.4 mm for the motion uncertainties and $\leq$0.8 mm/0.7° for the patient set-up uncertainties.

Conclusions: Average motion and patient set-up uncertainties during radiotherapy treatment were found to be limited. However, uncertainties were larger for the cranio-caudal direction and outliers were found in all orthogonal directions. When having available 4D-CT and CBCT information, the use of patient-specific and anisotropic safety margin expansions is advised for both target volume and OAR.

ARTICLE HISTORY
Received 4 November 2017
Accepted 6 February 2018

Introduction

Wilms' tumor (WT) is the most common malignancy of the kidney in childhood. By tailoring systemic agents, surgery and radiotherapy, overall survival of WT has been consistently high over the last decades [1,2]. Therefore, long-term toxicity of cancer treatment has become an important issue. In addition to treatment induced neoplasms [3], children undergoing abdominal radiotherapy are at increased risk of developing orthopedic, renal, metabolic, hepatic and vascular problems [4–6].

In the radiotherapy workflow, there are many possible sources of uncertainty that may limit the accuracy of the treatment such as (1) delineation (systematic), (2) motion (systematic and random) and (3) patient set-up (systematic and random) uncertainties. Delineation uncertainties are caused by inter-observer variability and to differences between image modalities (i.e. soft-tissue contrast). Motion uncertainties arise from displacements of the tumor bed (TB) and organs at risk (OAR) either caused by respiration (intra-fraction uncertainty) or by day-to-day variations like organ filling and weight changes (inter-fraction uncertainty). Patient set-up uncertainties result from patient positioning variations during treatment delivery (intra-fraction uncertainty) or in between fractions (inter-fraction uncertainty). As a consequence, safety margins should be used for both TB and OAR to assure adequate target coverage without exceeding healthy tissue dose constraints [7].

Motion and/or patient set-up uncertainties have already been studied for abdominal tumors in adults [8–10] and in children [11–18]. Four-dimensional computed tomography (4D-CT) [11,12] and 4D magnetic resonance imaging (MRI) [13] are used to estimate the breathing uncertainty and daily cone-beam CT-scans (CBCT) are used to assess both intra- and inter-fraction uncertainties [14–18]. However, none of these studies with pediatric patients has investigated both intra- and inter-fraction TB and OAR motion and patient set-up uncertainties for a homogeneous disease patient cohort at a single institute. A comprehensive assessment of uncertainties

CONTACT Filipa Guerreiro F.Guerreiro@umcutrecht.nl Department of Radiotherapy, University Medical Center Utrecht, Heidelberglaan 100, 3584 CX Utrecht, The Netherlands

Supplemental data for this article can be accessed here.

for abdominal target volumes is essential to take advantage of the state-of-the-art of radiotherapy treatment deliveries, such as intensity-modulated radiation therapy (IMRT), volumetric-modulated arc therapy (VMAT) and intensity-modulated proton therapy (IMPT). Thus, the purpose of this study was to analyze these uncertainties during image-guided radiation therapy (IGRT) in pediatric patients with WT undergoing flank irradiation using 4D-CT and daily CBCT-scans.

Material and methods

A flowchart with all steps of the pediatric radiotherapy chain at the Department of Radiation Oncology of the University Medical Center Utrecht (UMCU), Utrecht, The Netherlands, is represented in Figure 1. For each step included in the uncertainty analysis, a detailed explanation of the method used is described in the following sections.

Patient and treatment characteristics

After institutional review board approval (WAG/mb/17/008865), data from 15 consecutive patients (six males, nine females) with WT undergoing flank irradiation between April 2015 and October 2016 at the UMCU were included. The average patient age at the time of treatment was 4 years (range 1–8 years). After four to six weeks of induction chemotherapy, a nephrectomy with para-aortic lymph node sampling was performed. A right nephrectomy was performed for a total of eight patients while a left nephrectomy was performed for the remaining seven patients (Supplementary Table 1). During surgery, four titanium clips were placed at the superior (close to the diaphragm), lateral and medial (close to the vessels) and inferior (close to the ureter stump) tumor resection margins. The stability of the position of the surgical clips was verified during treatment by calculating the distance between the clips on the pre-treatment CBCT-scans. No signs of clip migration were observed.

Treatment preparation was performed under general anesthesia (GA) in ten out of the 15 patients. Furthermore, radiotherapy was delivered under GA for six out of the 15 patients due to limited patient compliance (Supplementary Table 1). A radiotherapy dose between 14.4 and 25.2 Gy was delivered to all patients using a 10 MV full-arc VMAT technique performed on an Elekta synergy linac equipped with an Agility multileaf collimator (Elekta, Stockholm, Sweden). The duration of the radiotherapy fractions, including imaging and irradiation, was on average 9 minutes.

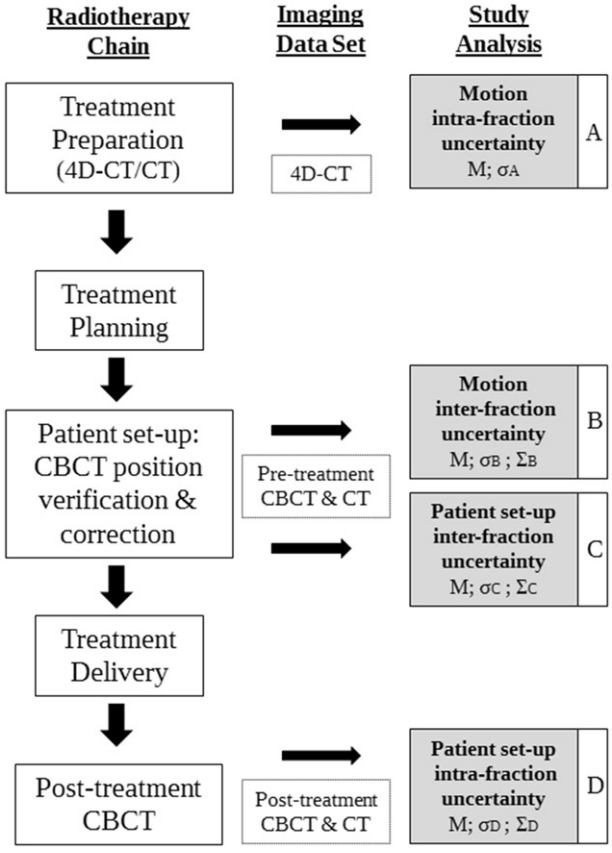

Figure 1. Radiotherapy treatment chain for pediatric patients at the Department of Radiation Oncology of the University Medical Center Utrecht (UMCU), Utrecht, The Netherlands, and the stages of motion and patient set-up uncertainties analysis (steps A–D) with the corresponding image modality used for the uncertainty assessment. The planning-CT was obtained by averaging the 4D-CT and was used for registrations with the CBCT-scans. Post-treatment CBCT-scans were only acquired for the first three to five fractions of each patient included in this study (Supplementary Table 1).

4D-CT and CBCT imaging: acquisition and registration

For each patient, all available imaging data, including a planning 4D-CT and daily CBCT-scans, were analyzed. Patients were fixated in a supine position in a vacuum mattress (Bluebag, Elekta, Stockholm, Sweden) with the arms wide along the body.

The 4D-CT-scans were obtained using a 16-, 40-, or 64-channel detector scanner (Brilliance, Philips Medical Systems, Best, The Netherlands) in spiral mode with the following parameters: 170 mAs/Slice, 120 kV, 0.44 s gantry rotation, 0.08 pitch, 1.5 mm collimation and 3 mm slice thickness. Each respiratory cycle during free-breathing was captured as a series of ten phases acquired at equally spaced intervals between 0% and 100%. Respiratory trace measurements for pulmonary gating were obtained using a deformable rubber belt fixed to the patient's chest (Philips Bellow System, Best, The Netherlands). Furthermore, the planning-CT was obtained by taking the pixel-by-pixel average of the ten phases of the 4D-CT. Both planning-CT and 4D-CT-scans shared the same spatial coordinates, thus no additional co-registration step was necessary.

Daily pre-treatment CBCT-scans were acquired for all treatment fractions using the Elekta XVI 4.5.1 on-board CBCT imaging system (Elekta, Stockholm, Sweden). Scans with an arc of 200° of 10 ms and 16 mA with 100 kV and an acquisition timeframe of 30 s, leading to four times less imaging dose than a standard adult pre-set, were taken. Each daily pre-treatment CBCT was co-registered to the planning-CT using the automatic rigid registration algorithm available clinically on the Elekta XVI software v5.0 [19,20]. Translational and rotational bone off-sets were obtained using a region of interest encompassing the vertebral column representative for the area in close proximity to the TB. Translational bone off-sets were corrected online using the automated

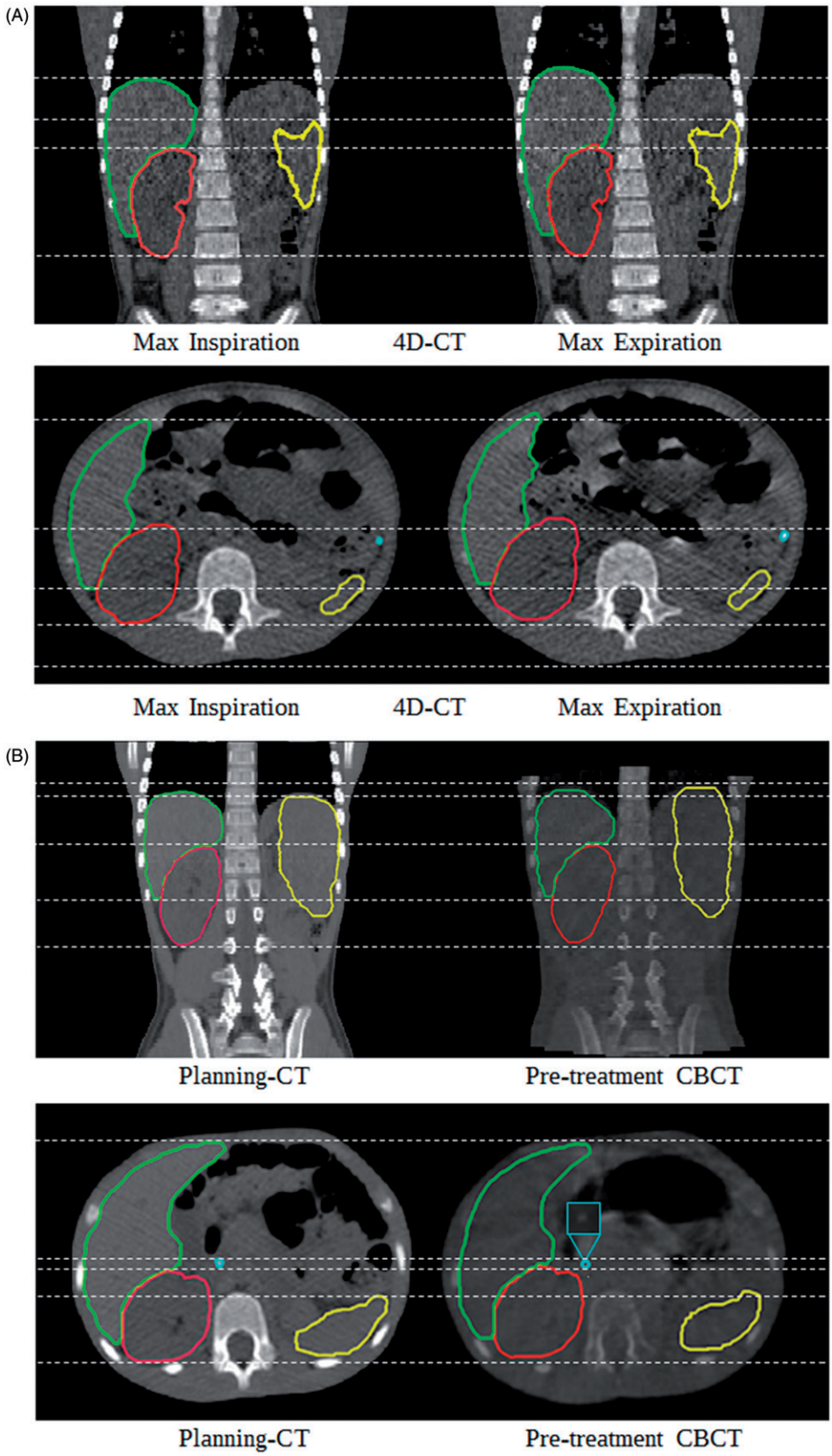

Figure 2. Examples of the imaging data sets used for the motion uncertainty assessment for both intra-fraction (A, top row) and inter-fraction (B, bottom row) uncertainties for one patient. Dashed lines are used to help to identify the borders of the delineated structures: liver, kidney, spleen and one surgical clip.

treatment table movement. Rotational bone off-sets were not directly corrected for and only when larger than 3°, in at least one direction, patient re-positioning was performed.

At our department, instead of the 10 mm planning target volume (PTV) margin around the clinical target volume (CTV), as recommended in the International Society of Paediatric Oncology (SIOP)-2001 protocol [21], a 5 mm margin is used around a patient-specific internal target volume (ITV). The ITV is used to account for the breathing uncertainty and is defined by visual inspection of the surgical clips motion on the 4D-CT.

As no information on intra-fraction patient set-up uncertainty was available for this patient cohort, to assess this uncertainty, post-treatment CBCT-scans were acquired for the first three to five fractions of each patient included in this study (Supplementary Table 1). The post-treatment CBCT-scans were co-registered to the planning-CT using the same procedure followed for the pre-treatment CBCT-scans. In total, 138 pre-treatment and 50 post-treatment CBCT-scans were analyzed (Supplementary Table 1).

Uncertainties assessment

Motion

Measurements of the motion uncertainties were done offline using the clinical registered images (as explained in section '4D-CT and CBCT imaging: acquisition and registration') and an in-house delineation software [22] (Figure 1, *steps A and B*). For the purpose of this study, the clips, liver, spleen, and contralateral kidney were delineated on the planning-CT by one radiation oncologist. TB and OAR motion uncertainties were quantified by center of mass (CoM) displacements, in all orthogonal directions, as this measure is less sensitive to organ deformation. The + and – signs indicate right/posterior/caudal and left/anterior/cranial directions, respectively. The individual displacements of the four surgical clips were used as surrogate for the assessment of the TB motion.

For the intra-fraction uncertainty estimation, the clips and OAR contours were translated/rotated from the planning-CT to match the anatomy of the maximum expiration and inspiration phases of the 4D-CT (Figure 2). Maximum inspiration and expiration phases of the 4D-CT were selected by visual inspection (Supplementary Table 1). Deviations in contours' boundaries (i.e. to remove the presence of air pockets from the inside of the contours) were corrected manually. Average volume differences between the defined contours on both 4D-CT phases were negligible (liver $\leq$4%, spleen $\leq$2%, kidney $\leq$1%). CoM displacements between the maximum expiration, used as a reference, and inspiration phases of the 4D-CT were calculated per patient.

For the inter-fraction uncertainty assessment, the clips and OAR contours were translated/rotated from the planning-CT to match the anatomy of the pre-treatment CBCT-scans (Figure 2). Deviations in contours' boundaries (i.e. due to different breathing phases) were corrected manually. Average volume differences between the planning-CT contours and the modified contours on the CBCT-scans were negligible (liver and spleen $\leq$6%, kidney $\leq$2%). CoM displacements between the planning-CT, used as a reference, and the pre-treatment CBCT-scans were determined for each patient.

Patient set-up

For the assessment of the patient set-up uncertainties, the clinical registered images (as explained in section '4D-CT and CBCT imaging: acquisition and registration') were used (Figure 1, *steps C and D*).

For the intra-fraction uncertainty assessment, the post-treatment CBCT-scans were used to calculate the translational and rotational bone off-sets with respect to the planning-CT for each patient [18]. Due to software reasons, the bone off-sets between the post-treatment CBCT-scans and the planning-CT, instead of the pre-treatment CBCT-scans, were used. Nevertheless, negligible differences in the bone off-sets in all orthogonal directions ($<$0.05 mm/0.3°) were observed between methodologies.

For the inter-fraction uncertainty assessment, the pre-treatment CBCT-scans were used to calculate the translational and rotational patient bone off-sets with respect to the planning-CT. During treatment, the alignment between the patient's planning and treatment position at the target volume location was achieved by applying online translational shifts to the treatment table (as explained in section '4D-CT and CBCT imaging: acquisition and registration'). Within the XVI software [20], rotational bone off-sets are converted into translational shifts resulting in a residual translational patient set-up uncertainty. The difference between the translational bone off-sets provided by the XVI software and the correction applied to the treatment table was used to estimate the translational inter-fraction patient set-up uncertainty.

Uncertainties analysis

Motion

For the intra-fraction uncertainty, the results are expressed as a group mean (M), as a range of values and as a group random error (σ_A; the standard deviation (SD) of the individual values of all patients) [7,23] (Figure 1, *step A*).

For the inter-fraction uncertainty, the results are expressed as an *M*, as a range of values, as a group systematic error (Σ_B; the SD of the individual means of all patients) and as a group random error (σ_B; root mean square (RMS) of the individual SDs) [7] (Figure 1, *step B*).

Patient set-up

For both intra- and inter-fraction uncertainties, the results are expressed as an *M*, as a range of values, as a group systematic ($\Sigma_{C,D}$; the SD of the individual means of all patients) and as a group random error ($\sigma_{C,D}$; RMS of the individual SDs) [7] (Figure 1, *steps C and D*).

Results

For the intra-fraction motion uncertainty, *M* was smaller than 0.8 mm for the TB (range: [−1.9;3.3] mm) and 3.2 mm for the

Table 1. Calculated group mean (M) and range results for the motion (steps A and B) and patient set-up (steps C and D) uncertainties. Steps A and D are related to the intra-fraction uncertainties and steps B and C to the inter-fraction uncertainties.

Error source	Evaluated structure		Measure	LR	AP	CC
A	TB (Clips)	Superior	*M* (mm)	−0.1	0.1	0.8
			Range (mm)	[−0.7; 0.7]	[−1.9; 1.5]	[0.0; 3.3]
		Lateral	*M* (mm)	0.0	0.3	0.8
			Range (mm)	[−1.2; 0.4]	[−0.5; 0.9]	[−0.3; 3.1]
		Medial	*M* (mm)	0.1	0.2	0.8
			Range (mm)	[−0.8; 1.3]	[−0.3; 1.1]	[−0.3; 2.5]
		Inferior	*M* (mm)	−0.2	0.2	0.4
			Range (mm)	[−1.1; 0.4]	[−0.4; 1.0]	[−0.8; 1.8]
	OAR	Kidney	*M* (mm)	0.0	0.1	0.6
			Range (mm)	[−0.5; 0.2]	[−0.7; 0.7]	[0.0; 3.2]
		Liver	*M* (mm)	−0.1	1.0	3.0
			Range (mm)	[−1.7; 1.6]	[0.5; 2.3]	[0.6; 4.7]
		Spleen	*M* (mm)	−1.3	0.9	3.2
			Range (mm)	[−3.4; 0.6]	[−0.1; 2.3]	[0.9; 5.5]
B	TB (Clips)	Superior	*M* (mm)	0.2	−0.5	1.0
			Range (mm)	[−3.6; 3.9]	[−4.6; 3.2]	[−3.2; 4.6]
		Lateral	*M* (mm)	0.2	−0.6	−1.1
			Range (mm)	[−3.8; 3.7]	[−5.5; 4.8]	[−6.9; 7.9]
		Medial	*M* (mm)	0.4	−0.6	−0.1
			Range (mm)	[−3.3; 3.8]	[−4.1; 4.7]	[−5.3; 3.3]
		Inferior	*M* (mm)	0.5	1.1	0.3
			Range (mm)	[−4.3; 3.9]	[−3.6; 4.2]	[−5.0; 5.0]
	OAR	Kidney	*M* (mm)	0.1	0.4	−0.2
			Range (mm)	[−3.7; 3.7]	[−1.6; 3.9]	[−5.6; 6.3]
		Liver	*M* (mm)	1.2	−0.1	−0.2
			Range (mm)	[−4.3; 4.0]	[−3.3; 4.8]	[−9.0; 8.1]
		Spleen	*M* (mm)	0.5	−0.2	−1.0
			Range (mm)	[−2.7; 3.5]	[−4.0; 4.9]	[−9.1; 9.6]
C	Bone off-set	Translational shift	*M* (mm)	0.1	−0.1	0.0
			Range (mm)	[−0.5; 0.7]	[−0.9; 0.8]	[−0.6; 0.6]
D	Bone off-set	Translational shift	*M* (mm)	0.0	−0.1	0.0
			Range (mm)	[−3.3; 2.0]	[−2.7; 3.2]	[−0.7; 4.8]
		Rotational shift	*M* (degree)	0.9	0.8	0.8
			Range (degree)	[0.0; 2.6]	[0.0; 2.8]	[0.0; 2.4]

LR: left-right; AP: anterior–posterior; CC: cranio-caudal; OAR: organs at risk; TB: tumor bed.

OAR (range: [−3.4;5.5] mm) in all orthogonal directions (Table 1 and Figure 3). σ_A was smaller than 1.4 mm (Table 2).

For the inter-fraction motion uncertainty, *M* was smaller than 1.1 mm for the TB (range: [−6.9;7.9] mm) and 1.2 mm for the OAR (range: [−9.1;9.6] mm) in all orthogonal directions (Table 1 and Figure 3). Σ_B and σ_B were smaller than 2.4 mm (Table 2).

The CoM displacements were more pronounced in the cranio-caudal (CC) direction for both intra- and inter-fraction motion uncertainties (Figure 3). Moreover, a large number of outliers in the TB and OAR CoM displacements were denoted between patients, especially for the inter-fraction motion uncertainty (Figure 3).

For the intra-fraction patient set-up uncertainty, *M* was smaller than 0.1 mm (range: [−3.3;4.8] mm) and 0.9° (range: [0.0°;2.8°]) in all orthogonal directions (Table 1). Σ_D and σ_D were smaller than 0.8 mm and 0.7°, respectively (Table 2). For the inter-fraction patient set-up uncertainty, *M* was smaller than 0.1 mm (range: [−0.9;0.8] mm) in all orthogonal directions (Table 1). Σ_C and σ_C were smaller than 0.2 mm (Table 2). Few outliers in both intra- and inter-fraction patient set-up uncertainties were detected between patients in all orthogonal directions.

Discussion

The purpose of this study was to quantify intra- and inter-fraction motion and patient set-up uncertainties during IGRT, using 4D-CT and daily CBCT-scans, in 15 patients with WT undergoing flank irradiation. Results demonstrate on average limited motion and negligible patient set-up uncertainties during treatment. However, a large number of outliers for the TB and OAR motion were found between patients, especially for the inter-fraction uncertainty.

For the motion uncertainties, average and maximum CoM displacements were always smaller than 8 mm in magnitude for the TB and 10 mm in magnitude for all OAR. Published studies have already reported the intra-fraction motion uncertainty for pediatric patients while calculating the CoM displacements between the maximum expiration and inspiration phases of 4D-CT [11,12] and 4D-MRI-scans [13]. For the TB, Uh et al. [13] quantified the breathing uncertainty for 17 patients younger than 8 years using 4D-MRI-scans. A larger average CoM displacement of the TB (1.6 mm versus maximum of 0.8 mm in the present study) was found by Uh et al., possibly due to the use of the whole CTV volume instead of the surgical clips to estimate the TB displacement. For WT patients undergoing flank irradiation after nephrectomy, the use of the CTV as surrogate for the TB motion uncertainty would be insufficient as the TB is not clearly discernible. Regarding the OAR, literature is available for the kidneys [11–13], spleen and liver [12,13]. Panandiker et al. [11] using 4D-CT-scans of a similar patient cohort (11 patients, range 2–8 years) reported slightly larger average CoM displacements of the kidney (1.9 mm versus 0.6 mm). The difference can be explained by the use of absolute

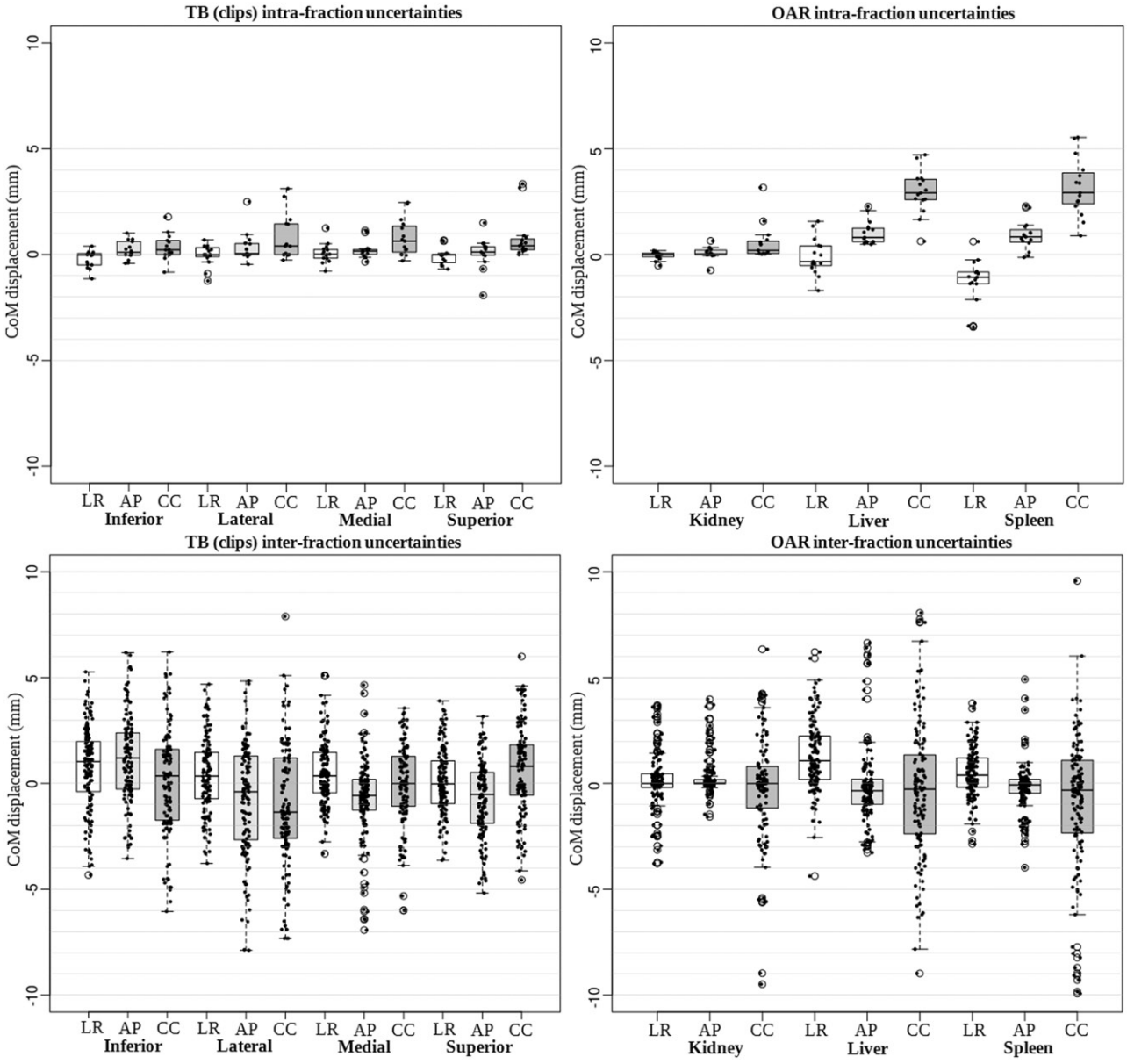

Figure 3. Boxplots with jitter describing the intra- (top row, step A) and the inter-fraction (bottom row, step B) center of mass (CoM) displacements of the tumor bed (TB) and organs at risk (OAR) for each orthogonal direction. Horizontal bar, boxes, whiskers, and circles represent median values, 50th and 90th percentiles and outliers, respectively. LR: left-right; AP: anterior–posterior; CC: cranio-caudal.

values of the CoM displacements by Panandiker et al. instead of considering the sign of the displacement as in the present study. With the purpose of calculating Σ and σ, the measured values and not their absolute values should be used [7]. Kannan et al. [12] found for 15 patients, while using 4D-CT-scans, an average CoM displacement in the CC direction, of 1.4, 2.5 and 3.1 mm for the kidney, liver and spleen, respectively. Uh et al. [13] reported an average CoM displacement in the CC direction of 1.6, 3.2 and 3.0 mm for the kidney, liver and spleen, respectively. The results observed in the present study (CoM displacements of 0.6, 3.0 and 3.2 mm for the kidney, liver and spleen, respectively) were comparable with the results from both publications [12,13].

Furthermore, published studies have already addressed the inter-fraction motion uncertainty of the CTV [16], kidneys [14,16] and the liver [16] but no data is available on the spleen. Nazmy et al. [16] looked at the CTV CoM displacements, using CBCT-scans of four neuroblastoma patients, and found a maximum displacement in the CC direction of 5 mm (versus 8 mm). Differences in the CoM displacements found can be explained by the differences in the methodology as Nazmy et al. used the whole CTV volume rather than the individual surgical clips for the TB motion uncertainty estimation. Huijskens et al. [14] observed an average kidney CoM displacement smaller than 1.5 mm (versus 0.6 mm) by using CBCT-scans of a heterogeneous group of 39 patients. The difference could be related to the considered patient population – mean age of 4 years in the present study and 8 years in Huijskens et al. study. Nazmy et al. [16] while using CBCT-scans of nine patients showed a maximum displacement in the CC direction of 10 mm (versus 6 mm) for the kidneys and 13 mm (versus 9 mm) for the liver. The use of the upper/lower pole of the organs for the measurements of the displacements by Nazmy et al., instead of the CoM,

Table 2. Calculated group systematic (Σ) and group random (σ) errors for the motion (steps A and B) and patient set-up (steps C and D) uncertainties. Steps A and D are related to the intra-fraction uncertainties and steps B and C to the inter-fraction uncertainties.

Error source	Evaluated structure		Error	LR	AP	CC
A	TB (Clips)	Superior	σ_A (mm)	0.4	0.7	1.0
		Lateral	σ_A (mm)	0.5	0.7	1.1
		Medial	σ_A (mm)	0.5	0.4	0.9
		Inferior	σ_A (mm)	0.4	0.4	0.6
	OAR	Kidney	σ_A (mm)	0.2	0.3	0.9
		Liver	σ_A (mm)	0.9	0.6	1.1
		Spleen	σ_A (mm)	1.1	0.7	1.4
B	TB (Clips)	Superior	Σ_B (mm)	1.1	1.2	1.1
			σ_B (mm)	1.2	1.3	1.7
		Lateral	Σ_B (mm)	1.4	2.0	2.2
			σ_B (mm)	1.2	1.8	1.9
		Medial	Σ_B (mm)	1.0	1.4	1.1
			σ_B (mm)	1.2	1.3	1.7
		Inferior	Σ_B (mm)	1.6	1.5	1.5
			σ_B (mm)	1.4	1.4	2.0
	OAR	Kidney	Σ_B (mm)	1.1	0.7	1.8
			σ_B (mm)	0.8	0.7	1.6
		Liver	Σ_B (mm)	0.8	1.7	2.4
			σ_B (mm)	1.5	1.1	2.2
		Spleen	Σ_B (mm)	0.7	0.8	2.4
			σ_B (mm)	1.0	0.9	2.4
C	Bone off-set	Translational shift	Σ_C (mm)	0.1	0.2	0.1
			σ_C (mm)	0.0	0.0	0.0
D	Bone off-set	Translational shift	Σ_D (mm)	0.5	0.4	0.4
			σ_D (mm)	0.7	0.8	0.8
		Rotational shift	Σ_D (degree)	0.6	0.5	0.4
			σ_D (degree)	0.6	0.6	0.7

LR: left-right; AP: anterior–posterior; CC: cranio-caudal; OAR: organs at risk; TB: tumor bed.

could explain the different results. The CoM displacements are less sensitive to deformations, thus Nazmy et al. might have interpreted organs deformations as translations while performing measurements with the upper/lower pole of the organs.

In the present study, the inter-fraction motion uncertainty was found to be larger when compared with the intra-fraction uncertainty. However, the inter-fraction uncertainty might be overestimated due to differences in the imaging procedures. Despite the negligible percentage of volume differences seen between contours delineated on the planning-CT and on the CBCT-scans ($\leq$6%), different image acquisition methods may still influence the baseline organ position, due to breathing, and the visibility of the organ boundaries, especially for the CBCT-scans due to poorer soft-tissue contrast.

The use of GA to immobilize patients during IGRT and patient-specific factors such as weight and height might also affect the TB and OAR motion uncertainties. Several studies in literature reported previously on this [11,12,14,15]. Panandiker et al. [11] found that the intra-fraction motion uncertainty of the kidney was smaller for patients treated with GA. They also concluded that renal motion had a significant correlation with the age and height of the patient. However, Kannan et al. [12] did not found significant differences in the intra-fraction motion uncertainty of the OAR between patients subgroups based on the use of GA and the patient age. Huijskens et al. reported that no significant correlations were found between the inter-fraction motion uncertainty of the kidney and height [14] and between the intra- and inter-fraction motion uncertainties of the diaphragm and patient-specific factors (age, height and weight) [15]. Moreover, for WT patients, the nephrectomy side might also influence the motion of the TB and the surrounding OAR. However, no data are available in the literature on this. In the present study, the relation between the intra- and inter-fraction TB and OAR motion uncertainties and the use of GA and nephrectomy side was analyzed using a non-parametric Mann–Whitney *U* test (data not shown). Significance differences were only found regarding the nephrectomy side (right versus left side) for the liver (average −1.1 versus 0.6 mm) and spleen (average −1.4 versus −0.4 mm) in the CC direction. Moreover, the correlation between the TB and OAR motion uncertainties and patient-specific factors (height and weight) was also determined using a Spearman's test (data not shown). No correlation was found between motion uncertainties and patient-specific factors. Despite the use of non-parametric statistical tests considering the small number of patients included in each subgroup ($n < 10$), a larger patient cohort is needed to confirm the results of the statistical significance between motion uncertainties and the use of GA, nephrectomy side and patient-specific factors.

Patient set-up uncertainties due to positioning variations were found to be small in this study and thus considered negligible when online CBCT imaging is employed and patients are immobilized supine in a vacuum mattress. Similar observations were done by Beltran et al. [18] regarding the intra-fraction patient set-up uncertainty. They reported an average uncertainty smaller than 0.5 mm (versus $\leq$0.1 mm) and Σ and σ smaller than 1 mm (versus $\leq$0.8 mm). For the evaluation of the intra-fraction patient set-up uncertainty, it must be noted that the post-treatment CBCT-scans were only acquired for the first fractions and using a modified CBCT pre-set compared with adults in order to reduce the imaging dose to the patient without compromising the

image guidance accuracy. As a result of the negligible patient set-up intra-fraction uncertainty observed, post-treatment CBCT-scans are currently not acquired at our department anymore.

The simultaneous assessment of both intra- and inter-fraction imaging data enabled an accurate estimation of the motion and patient set-up uncertainties during radiotherapy treatment of WT patients undergoing flank irradiation. For the motion uncertainties, due to the wide distribution of the Σ and σ (range 0.4–2.2 mm) and due to the large number of outliers found among the considered patient population in all orthogonal directions, the use of patient-specific and anisotropic target volume safety margins is recommended. The use of personalized target margins can limit the volume of healthy tissue included in the target volume allowing for the reduction of the risk of chronic toxicity. Assuming that children are at particular risk of developing radiation-induced late effects as they are more sensitive to radiation than adults, we advise the acquisition of both 4D-CT-scans during preparation and pre-treatment CBCT-scans during radiotherapy treatment for the assessment of the margin expansions. The 4D-CT-scans should be used for the definition of an individualized ITV to account for the breathing uncertainty. Moreover, TB motion should be assessed using the surgical clips displacements. Without the use of surgical clips, no estimation of the TB motion uncertainty for patients with WT would be possible. Furthermore, pre-treatment daily CBCT-scans should be acquired for both online correction of the patient position and visualization of eventual OAR displacements or some rare deformations with respect to the TB. However, despite CBCT imaging offers adequate bone contrast for patient positioning, the visualization of the target and OAR might be compromised due to poor soft-tissue contrast. MRI-guided treatment systems currently under development [24], which provide superior soft-tissue contrast allowing for adaptive radiotherapy regimes without patient radiation burden, are showing to be a great promise for optimal IGRT in the pediatric population, for whom there is particular concern for potential late effects related to the radiation dose and the risk of developing secondary cancer malignancies [25].

Loco-regional control rates exceeding 95% with radiotherapy doses between 14.4 and 25.2 Gy in children with WT should force clinicians towards better sparing of the OAR [1]. Taking into account that individual OAR motion uncertainties could go up to 10 mm, in addition to patient-specific and anisotropic target safety margins, to ensure an optimal sparing we recommend the use of patient-specific and anisotropic OAR safety margins individualized based on the 4D-CT and on the daily CBCT-scans if an adaptation is demanded.

To the author's knowledge, this is the first study evaluating both intra- and inter-fraction motion uncertainties of the OAR and TB, demarcated by surgical clips, and patient set-up uncertainties for a homogeneous disease patient cohort at a single institute. The gold standard for WT patients undergoing flank irradiation consists of using 10 mm margin around the CTV as recommended by the international SIOP-2001 protocol [21]. As this protocol was developed long before IGRT was implemented and as new RT approaches are under development, knowledge on the major uncertainties during radiotherapy treatment for WT patients is essential. Facing the limited average motion uncertainties, the negligible patient set-up uncertainties and the use of individualized margins based on the imaging modalities, such as 4D-CT and CBCT, the use of smaller safety margins than the one suggested by the SIOP-2001 protocol might be achieved. However, for the assessment of the universal PTV expansion to use for this patient category, an estimation of the delineation uncertainty and a larger patient cohort would be necessary. Future studies involve evaluating the effect of the use of patient-specific and reduced margins on the OAR doses using both conformal IGRT techniques and novelty techniques such as IMPT and MRI-guided treatments for abdominal pediatric cancer.

Conclusions

This study comprises an overview of uncertainties during radiotherapy treatment for a homogeneous group of children with WT undergoing flank irradiation. With the purpose of reducing safety margins, IGRT techniques are highly recommended for these patients. Imaging data collected before and during radiotherapy demonstrated limited TB and OAR motion and negligible patient set-up uncertainties. For the motion uncertainties, due to the wide distribution of the Σ and σ found and due to the existence of a large number of outliers among the considered patient population in all orthogonal directions, the use of patient-specific and anisotropic safety margin expansions can be recommended for both target and OAR when having available 4D-CT and daily CBCT information.

Disclosure statement

No potential conflict of interest was reported by the authors.

References

[1] Pritchard-Jones K, Bergeron C, de Camargo B, et al. Omission of doxorubicin from the treatment of stage II–III, intermediate-risk Wilms' tumour (SIOP WT 2011): an open-label, non-inferiority, randomised controlled trial. Lancet. 2015;386:1156–1164.

[2] de Kraker J, Graf N, van Tinteren H, et al. Reduction of postoperative chemotherapy in children with stage I intermediate-risk and anaplastic Wilms' tumour (SIOP 93-01 trial): a randomised controlled trial. Lancet. 2004;364:1229–1235.

[3] Taylor AJ, Winter DL, Pritchard-Jones K, et al. Second primary neoplasms in survivors of Wilms' tumour – a population-based cohort study from the British Childhood Cancer Survivor Study. Int J Cancer. 2008;122:2085–2093.

[4] van Waas M, Neggers S, Raat H, et al. Abdominal radiotherapy: a major determinant of metabolic syndrome in nephroblastoma and neuroblastoma survivors. PLoS One. 2012;7:522–537.

[5] Ritchey ML, Green DM, Thomas PRM, et al. Renal failure in Wilms' tumor patients: a report from the National Wilms' Tumor Study Group. Med Ped Oncol. 1996;26:75–80.

[6] Rate WR, Butler MS, Robertson WW, et al. Late orthopedic effects in children with Wilms' tumor treated with abdominal irradiation. Med Pediatr Oncol. 1991;19:265–268.

[7] van Herk M. Errors and margins in radiotherapy. Semin Radiat Oncol. 2004;14:52–64.

[8] Wysocka B, Kassam Z, Lockwood G, et al. Interfraction and respiratory organ motion during conformal radiotherapy in gastric cancer. Int J Radiat Oncol Biol Phys. 2010;77:53–59.
[9] Pham D, Kron T, Foroudi F, et al. A review of kidney motion under free, deep and forced-shallow breathing conditions: implications for stereotactic ablative body radiotherapy treatment. Technol Cancer Res Treat. 2014;13:315–323.
[10] van der Horst A, Wognum D, Davila Fajardo R, et al. Interfractional position variation of pancreatic tumors quantified using intratumoral fiducial markers and daily cone beam computed tomography. Int J Radiat Oncol Biol Phys. 2013;87:202–208.
[11] Pai Panandiker AS, Sharma S, Naik MH, et al. Novel assessment of renal motion in children as measured via four-dimensional computed tomography. Int J Radiat Oncol Biol Phys. 2012;82: 1771–1776.
[12] Kannan S, Teo BK, Solberg T, et al. Organ motion in pediatric high-risk neuroblastoma patients using four-dimensional computed tomography. J Appl Clin Med Phys. 2017;18:107–114.
[13] Uh J, Krasin MJ, Li Y, et al. Quantification of pediatric abdominal organ motion with 4-dimensional magnetic resonance imaging method. Int J Radiat Oncol Biol Phys. 2017;99:227–237.
[14] Huijskens SC, van Dijk IW, de Jong R, et al. Quantification of renal and diaphragmatic interfractional motion in pediatric image-guided radiation therapy: a multicenter study. Radiother Oncol. 2015;117:425–431.
[15] Huijskens SC, van Dijk IWEM, Visser J, et al. Magnitude and variability of respiratory-induced diaphragm motion in children during image-guided radiotherapy. Radiother Oncol. 2017;123: 263–269.
[16] Nazmy M, Khafaga Y, Mousa A, et al. Cone beam CT for organs motion evaluation in pediatric abdominal neuroblastoma. Radiother Oncol. 2012;102:388–392.
[17] van Dijk IW, Huijskens SC, de Jong R, et al. Interfractional renal and diaphragmatic position variation during radiotherapy in children and adults: is there a difference? Acta Oncol. 2017;10:1–7.
[18] Beltran C, Pai Panandiker AS, Krasin MJ, et al. Daily image-guided localization for neuroblastoma. J Appl Clin Med Phys. 2010; 11:3388.
[19] Borgefors G. Hierarchical chamfer matching: a parametric edge matching algorithm. *IEEE Trans Pattern Anal Machine Intell. 1988;10:849–865.
[20] Elekta AB. Elekta Synergy clinical user manual XVI R5.0. Stockholm: Elekta; 2013.
[21] De Kraker J, Graf N, Pritchard-Jones K, et al. Nephroblastoma clinical trial and study SIOP 2001, Protocol. SIOP RTSG; 2001.
[22] Bol GH, Kotte AN, van der Heide UA, et al. Simultaneous multimodality ROI delineation in clinical practice. Comput Methods Programs Biomed. 2009;96:133–140.
[23] van Herk M, Witte M, van der Geer J, et al. Biologic and physical fractionation effects of random geometric errors. Int J Radiat Oncol Biol Phys. 2003;57:1460–1471.
[24] Lagendijk JJ, van Vulpen M, Raaymakers BW. The development of the MRI linac system for online MRI-guided radiotherapy: a clinical update. J Intern Med. 2016;280:203–208.
[25] Hess CB, Thompson HM, Benedict SH, et al. Exposure risks among children undergoing radiation therapy: considerations in the era of image guided radiation therapy. Int J Radiat Oncol Biol Phys. 2016;94:978–992.